



## Switched Inductor Based Quadratic Boost Converter

Mr. Harsh Visakh V, PG Scholar

*Dept of Electrical & Electronics Engg,  
Mar Athanasius College of Engineering  
Kothamangalam, Kerala, India*

Prof. Kavitha Issac

*Dept of Electrical & Electronics Engg,  
Mar Athanasius College of Engineering  
Kothamangalam, Kerala, India*

Prof. Smitha Paulose

*Dept of Electrical & Electronics Engg,  
Mar Athanasius College of Engineering  
Kothamangalam, Kerala, India*

Prof. Eldhose K A

*Dept of Electrical & Electronics Engg,  
Mar Athanasius College of Engineering  
Kothamangalam, Kerala, India*

Prof. Neethu Salim

*Dept of Electrical & Electronics Engg,  
Mar Athanasius College of Engineering  
Kothamangalam, Kerala, India*

Prof. Linu Jose

*Dept of Electrical & Electronics Engg,  
Mar Athanasius College of Engineering  
Kothamangalam, Kerala, India*

**Abstract**—There is no pulsation in the converter's input current, and the inductor's current is low. The continuous conduction mode (CCM) converter's mathematical model and operating principle are described. Power loss and steady-state performance analyses are carried out for the converter. The converter's small-signal model is then obtained employing the state space averaging technique. The efficiency of the recommended converter can be raised by its low inductor current and voltage stress. As far as voltage gain requirements are concerned, the quadratic boost converter finds greater application than the boost converters. Using a conventional quadratic boost converter operating at a duty ratio to achieve high gain results in high efficiency and reduces voltage stress. Reduced voltage stress across the switches is achieved by modifying this structure by adding a switched inductor. MATLAB/SIMULINK R2020b is used to simulate the converter and produce the results. The presented circuit simulations and experiments validate the converter's good performance. A TMS320F28027F microcontroller is used to perform the hardware prototype, which has a 2V input and produces an output of 6.6V.

**Index Terms**—Boost Converter, Gain, Efficiency.

### I. INTRODUCTION

Photovoltaic (PV) power systems have seen a significant increase in popularity in recent years. Many PV markets throughout the world introduced solar photovoltaic technology to replace traditional energy sources. PV modules have the capability to function as either a standalone or isolated system when connected to the grid. Photovoltaic (PV) systems typically generate low voltage. Converters must be connected in order to raise the output voltage of PV systems and guarantee a steady voltage for the load or the grid's input side. As a result, DC-DC converters with a high voltage conversion ratio, high efficiency, affordable price, and small size are in high demand. Traditionally, step-up applications have used the boost converter. It is simple in structure and is inexpensive. But since it will put switching devices under a lot of voltage stress and reduce efficiency, obtaining high voltage gain at a very high duty ratio is not the best course of action [1].

DC-DC converters used for step-up applications also include isolated converters, such as half bridge, full bridge, fly back, and push-pull type converters. By modifying the turns ratio, these converters are capable of producing large gains [2]. This system has a number of drawbacks in spite of its benefits. These include the parasitic capacitance and leakage inductance that form in the secondary winding of the transformer, which cause high voltage stress across the switching devices as well as high voltage and current ripple. The system performance is further deteriorated by these factors, which increase switching losses because of high power dissipation and noise [3]. High gain can also be achieved with DC-DC converters with coupled inductors by varying the coupled inductor's turns ratio, and these converters are simpler to operate. However, the converter efficiency is reduced by leakage inductance losses and voltage spikes across the power switches when coupled inductors are used. The circuit becomes more complicated as a result of the need for additional snubber circuits [4] and [5].

Boost topologies can be cascaded to achieve high voltage gain in the simplest way possible. These converters are referred to as quadratic boost converters or cascade boost converters. However, cascaded structures will have a large number of stages. Therefore, it needs a lot of components, which ultimately results in a complicated circuit, low efficiency, and high cost [6]. In order to minimize the number of components, a quadratic converter is typically designed as a single switch converter [7]. However, because each boost cell's current flows into a single common switch, this method increases conduction and switching losses. Therefore, to increase power efficiency, soft-switching technology and a decrease in switch voltage are needed. For this reason, zero voltage switching, or ZVS, is used to increase power efficiency. The control circuit gets more complicated as a result, and an extra switch is needed [8]. By using a switched inductor or capacitor cell, voltage gain can also be increased. Discussed in [9] are various switched inductor and switched capacitor topologies. These are obtained

through the manipulation of the inductor and capacitor's series and parallel connections. But the switch is under high voltage stress, equal to the output voltage, and the voltage gain is restricted.

## II. METHODOLOGY

The Modified the switched inductor based quadratic boost converter consist of two switch (S1, S2), five diode (D1, D2, D3, D4 and D5), three inductor (L1, L2, L3) and two Capacitor (C1, C2) Figure 3.6 shows the Modified the switched inductor based quadratic boost converter.

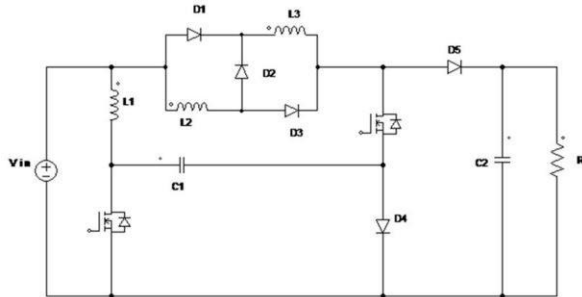


Fig. 1. switched inductor based quadratic boost converter

### A. Modes of Operation

The continuous conduction mode (CCM) and the continuous bidirectional conduction mode (CBCM) are the two primary operating modes of the suggested boost converter. The input inductor current,  $i_{L1}$ , flows continuously in one direction in both modes. The rear-inductor current  $i_{L2}$  operates differently in CCM and CBCM because it flows continuously in a unidirectional manner in CCM and a bidirectional fashion in CBCM.

1) *Mode 1:* At  $t = t_0$ , when Switches S1 and S2 are activated in this mode. D1, D3, and D5 are forward biased diodes, while D2, D4, and D5 are reverse biased. Three inductors, L1, L2, and L3, are charged by the input voltage source. In addition to feeding the load and providing current, the capacitor C2 also discharges C1. In the meantime, C2 is released to the load. Figure 2 shows operating circuit of mode 1.

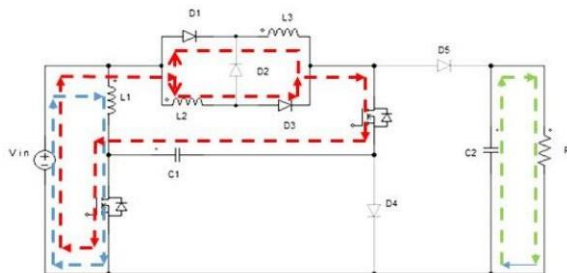


Fig. 2. Operating circuit of of Mode 1

2) *Mode 2:* At  $t = t_1$ , When in mode 2, both S1 and S2 are not in use. D1, D3, and D5 diodes are reverse biased, while D2, D4, and D5 diodes exhibit forward bias. Through the capacitor C1, the current flowing through inductors L1 discharges. Mode 2 sees the inductors L2 and L1 discharge through the load. According to their respective loads, the two capacitors are charging. Figure 3 shows the operating circuit of mode 2.

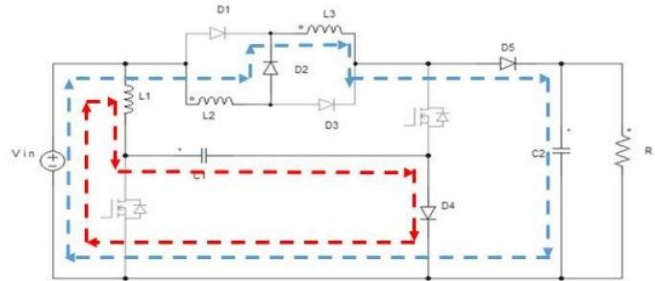


Fig. 3. Operating circuit of of Mode 2

Figure 4 shows the theoretical waveforms for mode 1 and mode 2.

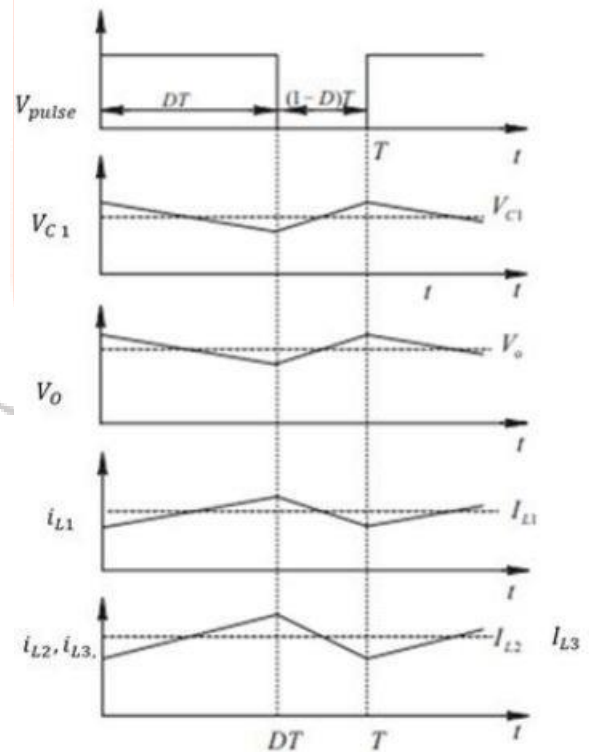


Fig. 4. Theoretical waveform

### B. Design of Components

$V_{in} = 20V$  is used as the input voltage.  $P_o = 24.5 W$  and  $V_o = 70V$  are used as the output power and output voltage, respectively.  $T_s = 1/f_s = 0.00002sec$  is the time period when the switches are operated with a duty ratio of  $D = 0.344$  and a switching frequency of  $f_s = 50kHz$ .

From the following equations, the inductors  $L_1$  are derived.

$$R_o = \frac{V_o^2}{P_o} = \frac{700^2}{24.5} = 200\Omega \quad (1)$$

Duty ratio,

$$\frac{V_o}{V_{IN}} = \frac{2D + 1 - D^2}{(1 - D)^2} = 3.5 \quad (2)$$

$$D = 0.344 \quad (3)$$

The following formulas are used to determine the inductors  $L_1$ .

$$I_{L1} = I_o * \frac{D}{(1 - D)^2} = 0.35 * \frac{0.344}{(1 - 0.344)^2} = 0.30A \quad (4)$$

$$L_1 \geq R_L * T * \frac{(1 - D)^4}{0.3} \quad (5)$$

$$L_1 \geq 200 * \frac{1 - 0.344^4}{0.09 * 50 * 10^3} \geq 1.9mH \quad (6)$$

It is approximated to 3 mH.

The following formulas are used to determine the inductors  $L_2$  &  $L_3$

$$I_{L1,L3} = \frac{I_o}{(1 - D)} = \frac{0.344}{(1 - 0.344)} = 0.53A \quad (7)$$

$$L_{2,3} \geq R_L * T * \frac{D * (2 - D)}{0.3} \quad (8)$$

$$L_{2,3} \geq \frac{200 * 0.344 * (2 - D)}{0.3 * 50 * 10^3} = 1.41mH \quad (9)$$

It is approximated to 3 mH.

Capacitors values are found from the following equations.

$$C_1 \geq \frac{D * T}{0.1 * R_L * (1 - D)^2} \quad (10)$$

The value of capacitor  $C_1$  set as  $10 \mu F$

$$C_2 \geq \frac{D * T}{0.001 * R_L} \quad (11)$$

$C_1$  and  $C_2$  is taken as  $100 \mu F$

TABLE I  
SIMULATION PARAMETERS OF QUADRATIC BOOST CONVERTER

Parameters	Value
Input voltage, $V_{in}$	20 V
Output voltage, $V_o$	70 V
Output load, R	200 $\Omega$
Switching frequency, $f_s$	50 kHz
Inductance( $L_1$ )	3mH, 2 A
Capacitance $C_1$	10 $\mu$ F, 45 V
Capacitance $C_2$	100 $\mu$ F, 100 V
Inductance( $L_2, L_3$ )	1.5mH, 1 A

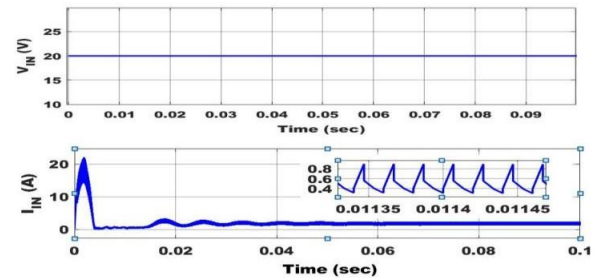


Fig. 5. (a) Input Voltage ( $V_{in}$ ) and (b) Input Current ( $I_{in}$ )

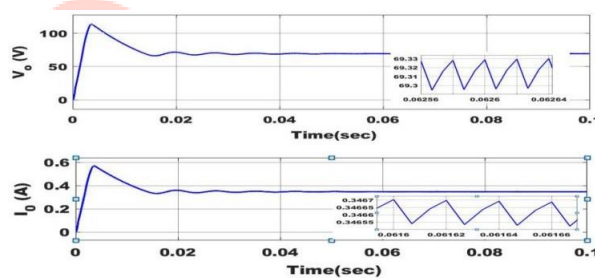


Fig. 6. (a) Output Voltage ( $V_o$ ) and (b) Output Current ( $I_o$ )

### III. SIMULATIONS AND RESULTS

In MATLAB/SIMULINK, the transformerless boost converter is simulated by selecting the parameters indicated in Table 1. With a steady switching frequency of 50 kHz, the switch is a MOSFET. A dc input voltage of 20 V results in a dc output voltage ( $V_o$ ) of 70 V when the output power ( $P_o$ ) is 24.5 W. The input voltage and current are shown in Figure 5, and the output voltage and current are shown in Figure 6. Consequently, the voltage gain is 6.6.

The gate pulse and voltage stress across the switch are displayed in Fig. 7a. The switch is under 31 V of voltage stress. The gate pulse and voltage stress across the switch are displayed in Fig. 8a. There is 70 V of voltage stress across the switch.

The Voltages across the capacitors  $V_{C1}$  and  $V_{C2}$  are shown in Fig. 9. The capacitor voltage of  $V_{C1}$  measured as 30.09V with 0.9V as voltage ripple. The capacitor voltage of  $V_{C2}$  measured as 69.23V with 0.04V as voltage ripple. Fig. 10 shows the current across Current through inductor  $IL_1$ , inductor  $IL_2$

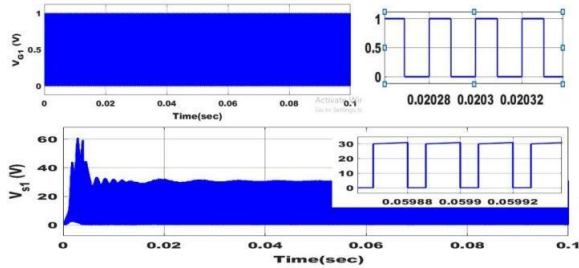


Fig. 7. Gate Pulse ( $V_{g1}$ ) and Voltage Stress ( $V_{s1}$ ) of switch S1

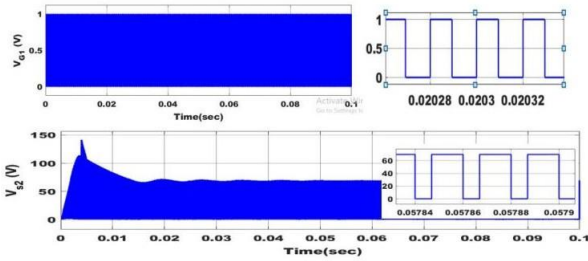


Fig. 8. Gate Pulse ( $V_{g2}$ ) and Voltage Stress ( $V_{s2}$ ) of switch S2

and inductor IL3. Current through inductor (IL1) is measured as 0.80A and the ripple current is 0.05A. Current through inductor (IL2) is measured as 0.51A with current ripple of 0.2A. Current through inductor (IL3) is measured as 0.67A with current ripple of 0.2A.

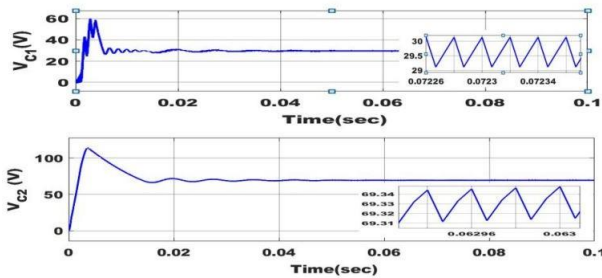


Fig. 9. Voltage across Capacitor (a) $V_{c1}$ , (b) $V_{c2}$

#### IV. PERFORMANCE ANALYSIS

The power output to input ratio determines a power equipment's efficiency at any load. This quadratic boost converter's efficiency vs. output power with R load and RL load is completed and displayed in Fig. 11. The switched inductor based quadratic boost converter has maximum efficiency for R and RL of 92.7% and quadratic boost converter has efficiency of 89.6%. Approximately 24.5 W is the medium power output variation in efficiency for both loads.

In figure 12, the gain of the quadratic boost converter is plotted as a function of duty ratio. The duty ratio can be changed to increase the gain.

In Figure 13, the output voltage ripple for a quadratic boost converter is plotted as a function of duty ratio.

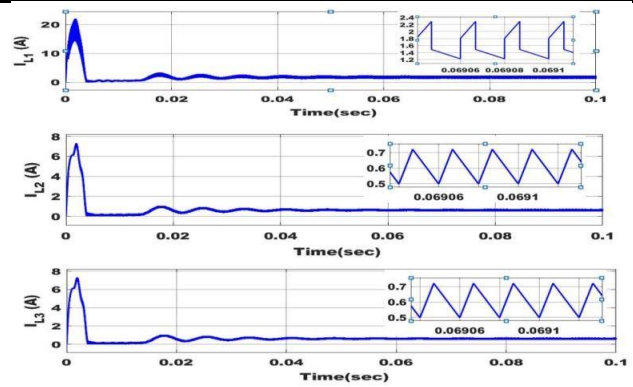


Fig. 10. Current across Inductance (a) $i_{L1}$ , (b) $i_{L2}$ , (c) $i_{L3}$

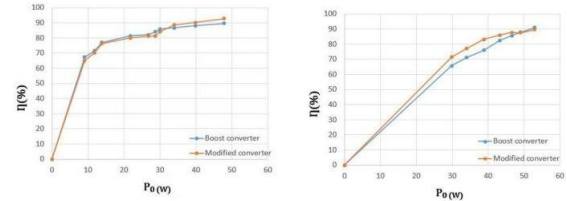


Fig. 11. Efficiency Vs Output Power for (a) R load (b) RL load

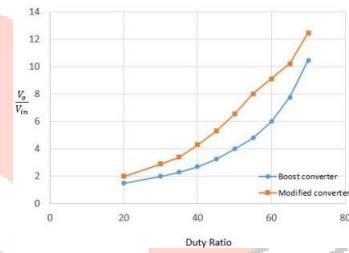


Fig. 12. Voltage gain VS Duty ratio

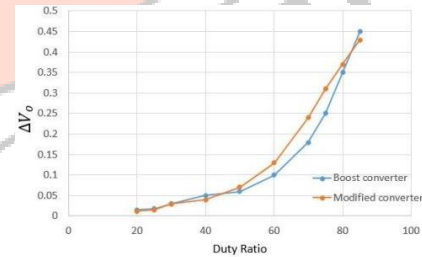


Fig. 13. Output Voltage Ripple VS Duty Ratio

Figure 14 displays the output voltage ripple for the modified boost converter plotted as a function of switching frequency. Increases in switching frequency result in a decrease in output voltage ripple.

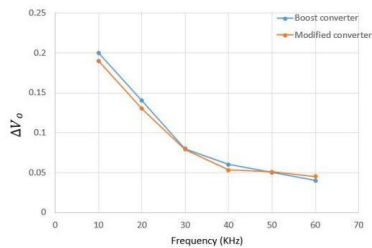


Fig. 14. Output voltage ripple VS frequency

V. COMPARITIVE STUDY

when  $V_{in} = 20V$ ,  $D=0.344$  power = 24.5 W and frequency is 50kHz. Here the number of components is high for switched inductor based quadratic boost converter and based quadratic boost converter is given in table 2. It is evident from the comparison that the gain increases from 3.4 to 6.8 when the input voltage and switching frequency are kept at the same values of 20 V and 50 kHz, respectively. With the modified converter, the voltage gain of the converter is also increased.

TABLE II

COMPARISON BETWEEN QUADRATIC BOOST CONVERTER AND SWITCHED INDUCTOR BASED QUADRATIC BOOST CONVERTER

Parameters	Modified Boost Converter	Quadratic Boost Converter
No. of switches	2	2
No. of Inductors	3	2
No. of Capacitors	2	2
No. of Diodes	5	2
Duty ratio	46.66	34.4
Frequency	50KHz	50KHz

A comparison of the enhanced gain boost converter and other converters, component by component, is presented in Table 3. Based on how many parts are utilized in various converters, comparisons are made. The Table shows that, out of all the converters, the enhanced gain converter uses the fewest large components.

TABLE III

COMPARISON BETWEEN QUADRATIC BOOST CONVERTER AND OTHER SIMILAR CONVERTER

Title	HSDC	MSBC	SIBC
No. of switches	1	2	1
No. of inductors	4	2	2
No. of capacitor	4	1	1
No. of diodes	8	5	4

VI. EXPERIMENTAL SETUP WITH RESULT

The input voltage is lowered to 2V for hardware implementation, and the TMS320F28335 processor is used to generate the switching pulses. The switch is a MOSFET IRF3205. The TLP250H optocoupler, which is used in the driver circuit, acts as a barrier to prevent external damage to the microcontroller as well as the gate required to activate the switches.

Fig. 15 illustrates the transformerless boost converter experimental setup. 2V of input with DC supply is provided by the DC source. The TMS320F28335 microcontroller provides switching pulses to the driver circuit. As a result, Fig. 16's power circuit yields an output voltage of 45 V. The converter's output voltage is obtained using a DSO oscilloscope.

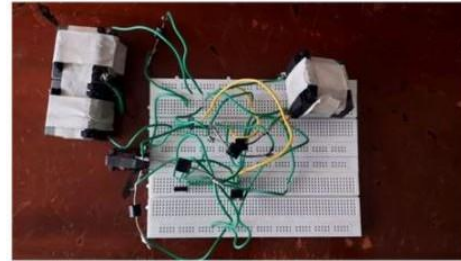


Fig. 15. Proposed Converter

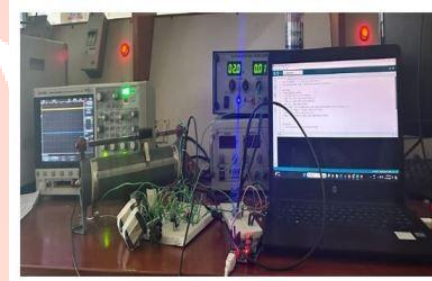


Fig. 16. Experimental Setup

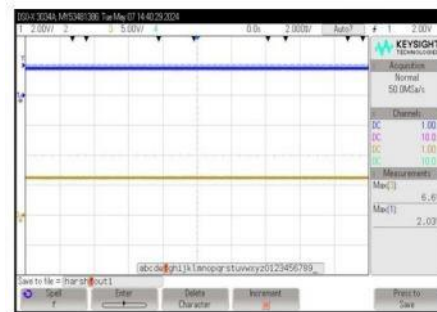


Fig. 17. Output Voltage of Proposed Converter

## VII. CONCLUSION

This paper introduces a novel switched inducer based on a quadratic boost converter. The following are some benefits of the suggested converter: This improves the converter's efficiency and lowers the copper losses in the inductors. The power switch's  $s_1$  is under relatively little voltage stress, the input current is constant, and the average inductor current is less than that. Under CCM, we have talked about steady state analysis and small signal modeling. The experiment's average current mode control generated 24.5 W of output power. The suggested converter can achieve 92 % efficiency at load. In order to improve the efficiency of the converter, two power switches will be soft-switched in later work.

## REFERENCES

- [1] Guanlin Li, Xin Jin, Xiyong Chen, and Xianmin Mu, "A Novel Quadratic Boost Converter With Low Inductor Currents", *CPSP transactions on power electronics and applications*, vol. 5, no. 1, march 2020 .
- [2] A. A. Fardoum and E. H. Ismail, "Ultra step-up DC-DC converter with reduced switch stress," *IEEE Transactions on Industry Applications*, vol. 46, no. 5, pp. 2025–2034, Sept. 2010.
- [3] Y. M. Ye and K. W. E. Cheng, "Quadratic boost converter with low buffer capacitor stress," in *IET Power Electronics*, vol. 7, no. 5, pp. 1162–1170, 2014, , vol. 7, no. 5, pp. 1162–1170, 2014.
- [4] M. G. Ortiz-Lopez, J. Leyva-Ramos, E. E. Carbajal-Gutierrez, and J. A. Morales-Saldana, "Modelling and analysis of switch-mode cascade converters with a single active switch," *IET Power Electronics*, vol. 1, no. 4, pp. 478–487, 2008.
- [5] F. Wang, "A novel quadratic boost converter with low current and voltage stress on power switch for fuel-cell system applications", *IEEE Transaction in Renewable Energy*, IEEE Transaction in Renewable Energy.
- [6] S. Ben-Yaakov and I. Zeltser, "The dynamics of a PWM boost converter with resistive input," *IEEE Transactions on Industry Applications*, vol. 46, no. 3, pp.613–619, 1996.
- [7] F. Blaabjerg, F. Iov, T. Kerekes, and R. Teodorescu, "Trends in power electronics and control of renewable energy systems," , *14th International Power Electronics and Motion Control Conference EPE-PEMC*, Ohrid, 2010, pp. K-1-K-19.
- [8] D. Sivaraj, M. Arounassalame, "High gain quadratic boost switched capacitor converter for photovoltaic applications", *Power Control Signals and Instrumentation Engineering (ICPCSI) 2017 IEEE International Conference*, 2017, pp. 1234–1239.
- [9] Q. Zhao, F. Tao, and F. C. Lee, "A front-end DC/DC converter for network server applications," *IEEE 32nd Annual Power Electronics Specialists Conference*, , pp. 1535- 1539, vol. 3, 2001.
- [10] M. Forouzesh, Yam P. Siwakoti, S. A. Gorji, F. Blaabjerg, and B. Lehman, "Step-Up DC–DC Converters: A Comprehensive Review of Voltage- Boosting Techniques Topologies and Applications", *IEEE Transactions on Power Electronics*, vol. 32, no. 12, pp. 9143–9178, 2017.

